On the description of the spray flame structure in a mixture fraction space

By A. Vié, B. Franzelli, B. Fiorina, N. Darabiha AND M. Ihme

1. Motivation and objectives

Spray combustion is of practical relevance to many industrial applications, including aeronautical combustors, automotive engines, and liquid rocket motors. In such systems, a liquid fuel is injected and atomized due to aerodynamic forces, generating a spray. The spray evaporates in the hot environment, mixes with an oxidizer stream, and eventually burns. Due to the evaporation process, spray flames are characterized by a strong inhomogeneous distribution of gaseous fuel (Luo *et al.* 2011). As a consequence, different combustion modes (premixed, partially-premixed, and diffusion) coexist in the flame (Sirignano 1983; Hollmann & Gutheil 1998). Therefore, complex modeling of the complex spray flames is of primary importance for applications, impacting relevant phenomena of the system (efficiency, pollutant emissions, extinction, stabilization), and is even more challenging compared to pure gaseous flames.

Classically, the structure of laminar gaseous diffusion flames is studied in the composition space defined by a passive scalar, called mixture fraction, in order to separately treat mixing and combustion.

The goal of the present work is to investigate the possibility of using a passive scalar to describe the structure of spray flames. In Section 2, the modeling framework is presented as well as the classical structure of counterflow spray flames. In Section 3, it is shown that its representation is not possible using the classical definition of the mixture fraction based on mass fraction of gaseous carbon atoms due to its non-monotonic behavior for spray flames. A new mixture fraction, which is based on carbon atoms of both liquid and gaseous phases, is defined in Section 4. Modeling assumptions to obtain a monotonic mixture fraction are also discussed . The impact of such modeling assumptions on the flame structure is investigated in Section 5. Conclusions about the usefulness of such a definition are discussed in Section 6.

2. Modeling Framework and test case

2.1. *The laminar counterflow spray flame*

In the present work, we consider the axisymmetric laminar counterflow spray flame, represented in Figure 1. Pure fresh air is injected from the left side (superscript ox) against a stream consisting of air and spray (superscript f). The axial gas phase velocities are identical at both injection sides: $v_g^{ox} = -v_g^f$. The axial velocities of the gas and liquid phases at the right injection are equal $v_g^f = v_l^f$.

One-dimensional flame simulations are performed with the REGATH counterflow code (Darabiha & Candel 1992). Liquid kerosene, modeled by $C_{10}H_{22}$, is considered. The chemistry is described using the BFER reduced mechanism of Franzelli *et al.* (2010) which takes into account 6 species and 2 reactions. According to this chemistry, a unity Lewis number is assumed for all gaseous species.

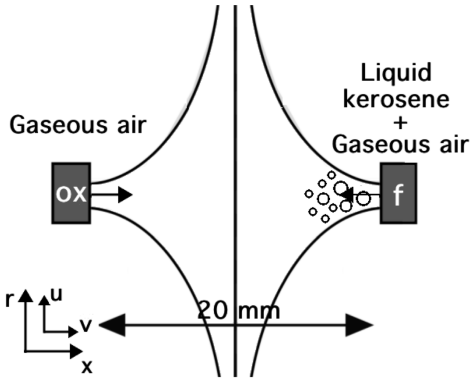

FIGURE 1. Schematic of the laminar counterflow spray flame.

2.2. *Governing equations*

The following transport equations for radial and axial momentum, enthalpy h_g, and species mass fractions Y_k are solved for the gaseous phase along the jet axis of the counterflow (Darabiha *et al.* 1993; Franzelli *et al.* 2013):

$$2\rho_g U_g + \frac{\partial \rho_g v_g}{\partial x} = n_l \dot{m}_l, \tag{2.1}$$

$$\rho_g U_g^2 + \rho_g v_g \frac{\partial U_g}{\partial x} = \frac{\partial}{\partial x}\left(\mu_g \frac{\partial U_g}{\partial x}\right) + J + n_l \dot{m}_l (U_l - U_g) - n_l \frac{f_r}{r}, \tag{2.2}$$

$$\rho_g v_g \frac{\partial h_g}{\partial x} = \frac{\partial}{\partial x}\left(\frac{\lambda_g}{c_{p_g}} \frac{\partial h_g}{\partial x}\right) + n_l \dot{m}_l (h_{F,g} - h_g) - n_l \dot{m}_l q, \tag{2.3}$$

$$\rho_g v_g \frac{\partial Y_k}{\partial x} = \frac{\partial}{\partial x}\left(\frac{\lambda_g}{c_{p_g}} \frac{\partial Y_k}{\partial x}\right) + W_k \dot{\Omega}_k + (\delta_{kF} - Y_k)\, n_l \dot{m}_l, \tag{2.4}$$

where μ_g is the mixture viscosity, λ_g is the thermal conductivity, v is the axial velocity, U is the radial reduced velocity, $\dot{\Omega}_k = \dot{\omega}_k / W_k$ is the molar chemical production rate of the k^{th} species, δ_{kF} is the Dirac's delta equal to one only for $k = F$ (where subscript F is the index for fuel species), λ_g and c_{p_g} are the heat conductivity and capacity of the gas phase, and $h_{F,g}$ is the gaseous enthalpy of the fuel species and q is the heat transfer between the gas and liquid phases. n_l is the droplet number density, $\dot{m}_l$ is the evaporation source term, and f_j is the j^{th} component of the drag force. Summation is implied only over i and j indices. Subscripts g and l denote the gaseous and the liquid phase, respectively. The system of equations is completed by imposing a constant radial pressure gradient in the axial direction: $\frac{1}{r}\frac{dP}{dr} = J$ and $\frac{dJ}{dx} = 0$.

The spray flow is described by the following Eulerian conservation equations (Darabiha

et al. 1993; Franzelli *et al.* 2013):

$$v_l \frac{\partial m_l}{\partial x} = -\dot{m}_l, \tag{2.5}$$

$$m_l U_l^2 + m_l v_l \frac{\partial U_l}{\partial x} = \frac{f_r}{r}, \tag{2.6}$$

$$m_l v_l \frac{\partial v_l}{\partial x} = f_x, \tag{2.7}$$

$$m_l c_{p_l} v_l \frac{\partial T_l}{\partial x} = \dot{m}_l (q - L), \tag{2.8}$$

$$2 n_l U_l + \frac{\partial n_l v_l}{\partial x} = 0, \tag{2.9}$$

where L is the latent heat of vaporization, c_{p_l} is the liquid heat capacity, R_l is the droplet radius, and m_l is the mass density of one droplet.The mass vaporization rate of a single droplet $\dot{m}_l$ is modeled by the expression for a spherically symmetric single-component droplet, using the following film temperature model (Spalding 1953; Kuo 1986):

$$\dot{m}_l = 4\pi R_l \rho_g D_{g,F} \ln(1 + B_M), \tag{2.10}$$

where $D_{g,F}$ is the diffusivity of the species being vaporized. B_M is the Spalding transfer number:

$$B_M = \frac{Y_{rs} - Y_F}{1 - Y_{rs}}, \tag{2.11}$$

where Y_{rs} is the saturated fuel mass fraction:

$$Y_{rs} = \sum_{k \neq F} \frac{(1 - X_{rs})}{(1 - X_F) W_F X_{rs}} Y_k, \tag{2.12}$$

with $X_{rs} = K_0 \exp(T_g)/P$.

The heat transferred from the gas to each droplet q is given by (Spalding 1953; Kuo 1986):

$$q = \frac{c_{p,g,F}}{B_T} (T_g - T_l), \tag{2.13}$$

where the heat transfer number B_T is here equal to B_M due to the unity Lewis number assumption. The i^{th} component of the drag f_i is modeled by the Stokes law:

$$f_i = \pi C_D R_l^2 \frac{1}{2} \rho_g (u_{g,i} - u_{l,i}) |u_{g,i} - u_{l,i}| = \frac{u_{g,i} - u_{l,i}}{\tau_p}, \tag{2.14}$$

where $C_D = 24/Re_D$ is the drag coefficient, Re_D is the droplet Reynolds number, and τ_p the relaxation time of the droplets.

2.3. *Spray flame structure*

In the following we consider the reference flame, characterized by the boundary conditions listed in Table 1 (case REF). Temperature and species mass fraction profiles are plotted in Figure 3. Results for the liquid volume fraction $\alpha_l = n_l \pi D_l^3/6$ and the droplet diameter are shown in Figure 3. Liquid kerosene evaporates near the right injection until it reaches the preheat flame region , where the evaporation drastically increases due to the higher gaseous temperature. The flame structure presents a first rich premixed reaction zone, where fuel reacts with the air injected from the right side. Since the equivalence ratio at

TABLE 1. Operating conditions.

Case name	T_g^f [K]	T_l^f [K]	D_l^f $[\mu m]$	α_l^f [-]	v_g^f $[m/s]$
REF	400	400	40	$3.4\ 10^{-4}$	0.20
SMALL	400	400	20	$3.4\ 10^{-4}$	0.20
LARGE	400	400	60	$3.4\ 10^{-4}$	0.20

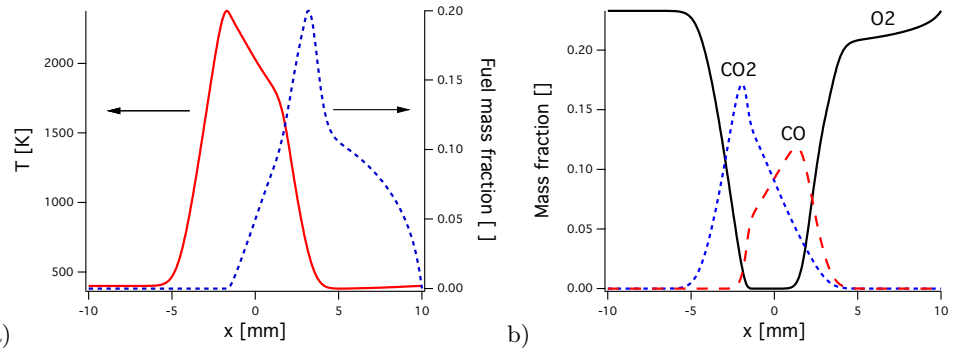

FIGURE 2. Profiles of the case REF as a function of axial position: a) gas temperature (full red line), fuel mass fraction (blue dashed line), and b) mass fraction of O2 (black full line), CO (red dashed line) and CO2 (blue dotted line).

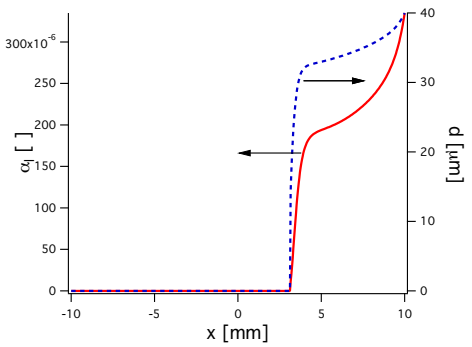

FIGURE 3. Profiles of the liquid volume fraction (full dashed line) and droplet diameter (dashed blue line) for case REF.

injection $\phi_{inj} = \dot{m}^F_{F,inj}/\dot{m}^F_{O,inj}$ is rich, all the oxidizer is consumed. A second diffusion-like reaction zone is observed near the left due to the recombination of the unburnt gas and products of the premixed region, with the fresh air provided by the oxidizer side.

3. Describing spray flame structure in mixture fraction space

Diffusion flames can be studied in the mixture fraction. This quantity, monotonically decreasing from the fuel side to the oxidizer side, represents the mixing between both streams. The mixture fraction can be defined with respect to an elemental mass fraction

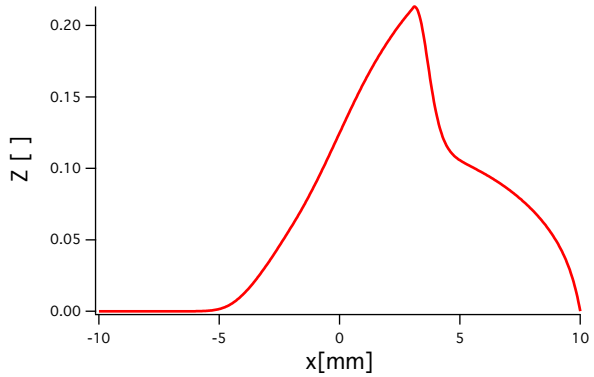

FIGURE 4. Gaseous mixture fraction for the case REF versus axial position.

that is present in the fuel (Bilger 1988), for example carbon:

$$Z_g = \frac{W_F}{n_{C,F} W_C} \sum_{k=1}^{N_{spec}} n_{C,k} \frac{Y_k W_C}{W_k}, \tag{3.1}$$

where W_k is the molar mass of the species k, W_C is the molar mass of carbon atoms, and $n_{C,k}$ is the number of carbon atoms in species k. In the case of a purely gaseous flame at unity Lewis number, the equation for the passive scalar Z_g is:

$$\frac{\partial(\rho_g v_g Z_g)}{\partial x} = \frac{\partial}{\partial x}\left(\frac{\lambda_g}{c_{p_g}} \frac{\partial Z_g}{\partial x}\right), \tag{3.2}$$

which guarantees the monotonicity of Z_g and a bijective relation between the axial position and the mixture fraction in a 1D laminar diffusion flame.

When it comes to spray flames, Z_g follows the equation:

$$\frac{\partial(\rho_g v_g Z_g)}{\partial x} = \frac{\partial}{\partial x}\left(\frac{\lambda_g}{c_{p_g}} \frac{\partial Z_g}{\partial x}\right) + n_l \dot{m}_l, \tag{3.3}$$

containing a source term due to the evaporation rate.The mixture fraction for the REF flame is plotted in Figure 4.The mixture fraction for a counterflow spray flame is no longer monotonic: at the fuel side, it is zero because all fuel is in liquid form. Then, it evaporates, leading to an increase of Z_g. Finally, when all the liquid fuel is evaporated, the mixture fraction monotonically decreases to zero at the oxidizer side. As this mixture fraction is no longer monotonic, it is inadequate for a coordinate transformation for two reasons:

(a) the solution in this mixture fraction space is not unique for a given mixture fraction (see Figure 5),

(b) the derivatives with respect to the mixture fraction are infinite at the inflection point(s) of the mixture fraction.

Therefore the classical gaseous mixture fraction tool cannot be used to study and identify spray flame structure, as this structure cannot be uniquely described in this space.

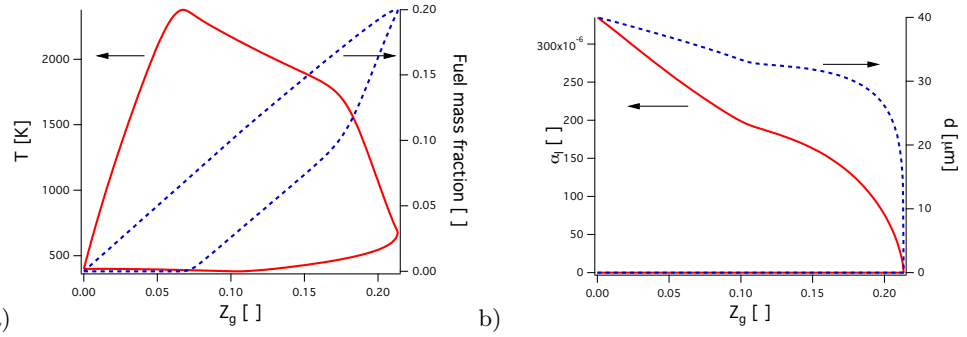

FIGURE 5. Profiles for the case REF as a function of the mixture fraction: a) gas temperature (full red line), fuel mass fraction (dashed blue line); b) liquid volume fraction (full red line), and droplet diameter (dashed blue line).

4. Definition of a monotonic mixture fraction

4.1. *Consideration of liquid fuel mass fraction in the mixture fraction definition*

The classical gaseous mixture is not suitable to describe spray flames due to its non-monotonicity. The objective here is to define a new mixture fraction to describe spray flames. A formulation of the mixture fraction could be introduced to take into account the liquid carbon atoms †. This total mixture fraction Z_t is:

$$Z_t = Y_F^L + \frac{W_F}{n_{C,F} W_C} \sum_{k=1}^{N_{spec}} n_{C,k} \frac{Y_k W_C}{W_k}, \tag{4.1}$$

where $Y_F^L = n_l m_l / \rho_g$. This definition is similar to the one proposed by Bilger (2011). Y_F^L follows the equation:

$$\frac{\partial \rho_g Y_F^L v_l}{\partial x} = -n_l \dot{m}_l \tag{4.2}$$

$$\frac{\partial \rho_g Y_F^L v_g}{\partial x} = -n_l \dot{m}_l - \frac{\partial}{\partial x_i} \left[\rho_g Y_F^L (v_l - v_g) \right] \tag{4.3}$$

Then, combining Eq. (4.6) and Eq. (3.3), the equation for Z is given by:

$$\frac{\partial \rho_g Z_t v_g}{\partial x} = \frac{\partial \rho_g Z_g v_g}{\partial x} + \frac{\partial \rho_g Y_F^L v_g}{\partial t} \tag{4.4}$$

$$\frac{\partial \rho_g Z_t v_g}{\partial x} = \underbrace{\frac{\partial}{\partial x} \left(\frac{\lambda_g}{c_{p_g}} \frac{\partial Z_t}{\partial x} \right)}_{Z_g \text{ diffusion}} - \underbrace{\frac{\partial}{\partial x} \left(\frac{\lambda_g}{c_{p_g}} \frac{\partial Y_F^L}{\partial x} \right)}_{Y_F^L \text{ differential diffusion}} - \underbrace{\frac{\partial}{\partial x} \left[\rho_g Y_F^L (v_l - v_g) \right]}_{\text{slip velocity}}, \tag{4.5}$$

where the Z_g-diffusion term comes from the fact that gaseous species diffuse, the Y_F^L differential diffusion is due to the absence of diffusion in the liquid phase, and the slip velocity term is due to the velocity difference between the two phases. Compared to Z_g, Z_t is non-zero at the fuel side injection and is not directly affected by the evaporation. Thus, this definition is a suitable candidate for a monotonic mixture fraction. However, compared to Eq. (3.3) which is valid only for gaseous flames, the additional

† The mixture fraction has to be based on an element of the fuel because other elements have the same values in both streams, leading to a non-monotonic mixture fraction definition.

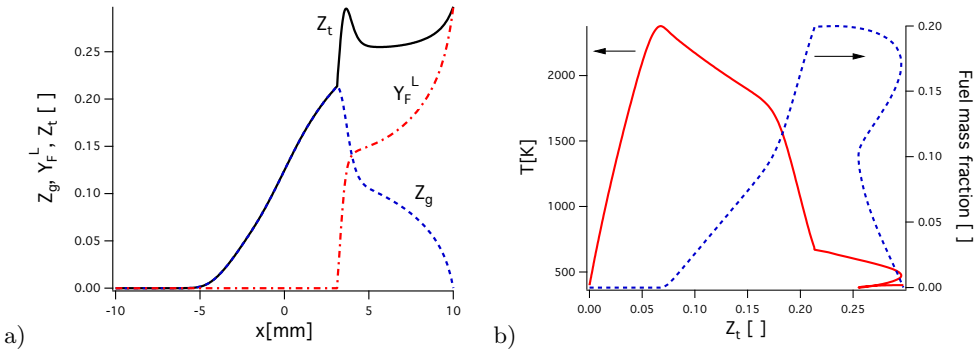

FIGURE 6. Case REF: a) Total mixture fraction (full black line), gaseous mixture fraction (dashed blue line) and liquid mass fraction (dotted red line); b) gas temperature (full red line) and fuel mass fraction (dashed blue line).

terms in Eq. (4.5) do not guarantee the monotonicity, and we need to verify whether this monotonicity would be preserved. The total mixture fraction, gaseous mixture fraction, and liquid fuel mass fraction profiles are plotted in Figure 6, along with solutions for temperature and fuel mass fraction against Z_t. Even by taking into account all carbon atoms, Z_t is not monotonic. The temperature and fuel mass fraction are represented as a function of Z_t in Figure 6b. The solution has multiple values for a given Z_t. In the following, model approximations are investigated in order to derive a conserved scalar mixture fraction formulation.

4.2. *Equilibrium liquid phase and equal diffusivity equations*

Considering Eq. (4.5), the only two terms that can break the monotonicity are the slip velocity term $-\partial_x \rho Y_F^L (v_l - v_g)$ due to the relaxation time of the droplets and the differential diffusion term $-\partial_x \left(\frac{\lambda_g}{c_{p_g}} \partial_x Y_F^L \right)$ because droplets do not diffuse.

To discard the effect of the slip velocity term, we consider a momentum equilibrium assumption, i.e., the liquid velocity is the same as the gas velocity. This assumption is valid for small droplets in the very small Stokes number limit. Then, the equation for the liquid mass fraction reduces to:

$$\frac{\partial \rho_g Y_F^L v_g}{\partial x} = -n_l \dot{m}_l, \tag{4.6}$$

and the resulting Z_t equation is then:

$$\frac{\partial \rho_g Z_t v_g}{\partial x} = \frac{\partial}{\partial x} \left(\frac{\lambda_g}{c_{p_g}} \frac{\partial Z_t}{\partial x} \right) - \frac{\partial}{\partial x} \left(\frac{\lambda_g}{c_{p_g}} \frac{\partial Y_F^L}{\partial x} \right). \tag{4.7}$$

Compared to the passive scalar equation Eq. (3.3), this equation still presents the negative differential diffusion term. To discard the effect of differential diffusion as well, we also investigated an equal diffusivity approximation. Unity Lewis number has been considered until now for all gaseous species, whereas the liquid mass fraction Y_F^L does not diffuse, i.e., $\mathrm{Le}^L = \infty$. Definition (4.5) then presents the same monotonicity problem as a gaseous flame when using species differential diffusion. In order to overcome this issue, the unity Lewis number of Y_F^L is introduced in an ad hoc way by adding a diffusion term

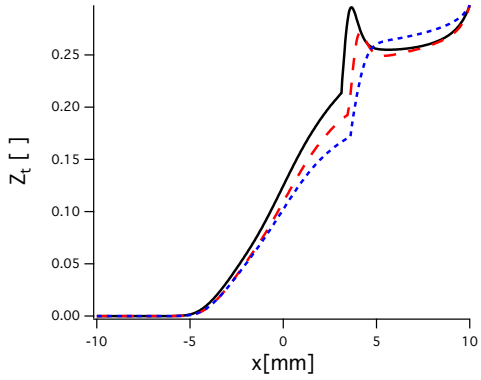

FIGURE 7. Case REF: total mixture fraction versus position for full (full black line), equilibrium (red dashed line) and equal diffusivity (blue dotted line) models.

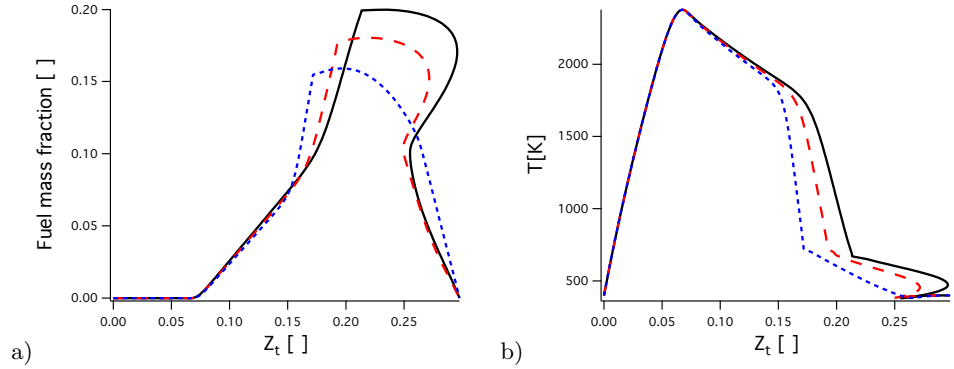

FIGURE 8. Case REF: a) fuel mass fraction and b) gas temperature versus total mixture fraction for full (black full line), equilibrium (red dashed line) and species-like (blue dotted line) models.

$\partial_{x_i}\left(\rho_g D \partial_{x_i} Y_F^L\right)$ to Eq. (4.6):

$$\frac{\partial \rho_g Y_F^L v_g}{\partial x} = \frac{\partial}{\partial x}\left(\frac{\lambda_g}{c_{p_g}}\frac{\partial Y_F^L}{\partial x}\right) - n_l \dot{m}_l. \tag{4.8}$$

The resulting equation for Z_t is then:

$$\frac{\partial \rho_g Z_t v_g}{\partial x} = \frac{\partial}{\partial x}\left(\frac{\lambda_g}{c_{p_g}}\frac{\partial Z_t}{\partial x}\right), \tag{4.9}$$

which is the classical formulation of a conserved scalar. The total mixture fraction resulting from each model is plotted in Figure 7. It is shown that the equilibrium model is not sufficient to guarantee the monotonicity of the mixture fraction, whereas the equal diffusivity approximation can. The results in the mixture fraction space confirm this statement, since only the equal diffusivity approximation solution is not multi-valued, (see Figure 8). Thus, only this model can be used to investigate flame structure in the mixture fraction space. However, the equilibrium assumption and the added diffusion term on which it relies are not satisfied for generic spray flames. Using comparisons with the full model solution, we next examine the impact of the simplified model approximations on the flame-structure representation.

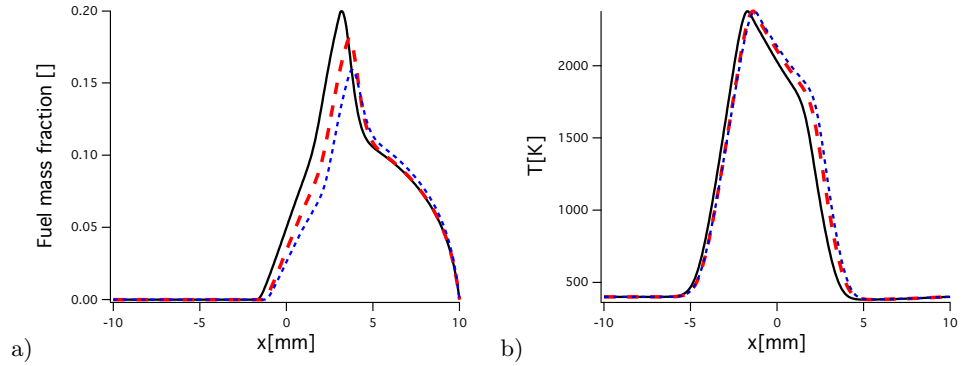

FIGURE 9. Case REF: a) fuel mass fraction and b) gas temperature as a function of the position for full (black full line), equilibrium (red dashed line), and equal diffusivity (blue dotted line) models.

5. Effect of model approximations on flame structure

In this section, we investigate the impact of the modeling assumptions that enable formulation of a monotonic mixture fraction. The goal is to understand the conditions under which the equal diffusivity approximation could be used to study spray flames. Three spray flames are considered by varying the droplet diameter at injection.

5.1. *Reference flame*

Solutions of each model for the reference flame are plotted in Figure 9 and 10. Both equilibrium and equal diffusivity assumptions affect the solution, shifting the reaction zone closer to the fuel side. Moreover, the maximum fuel mass fraction is smaller than that of the full model for each simplified model, with an error close to 25% for the equal diffusivity approximation, the model at which the errors due to equilibrium assumption and additional diffusion term accumulate. The position at which all droplets have disappeared is also affected by these assumptions, shifting it towards fuel injection. In Figure 11, the radial flux $n_l U_l$, the axial flux $\partial_x n_l v_l$, and the additional diffusion are plotted as a function of x-position. This confirms that the diffusion term has an impact on the solution at the injection and location of droplets, although this effect is negligible elsewhere.

5.2. *Small diameter*

The equilibrium assumption is valid for small droplets. We investigate a case where droplets are injected at a diameter of 20 μm, keeping the mass flow rate the same as for the reference flame (case SMALL in Table 1). Results are plotted in Figs. 12-14. First, we verify that the equal diffusivity model is the only model with a monotonic mixture fraction. For the gas phase, all models give equivalent results, but in the liquid phase, the equal diffusivity approximation has a great effect on the solution. The flame structure is not affected by these discrepancies because all droplets vaporize within a short distance after entering the first flame front. Compared to the reference case, where this model did not greatly affect the liquid phase, here the additional diffusion term has a significant impact on the solution, as shown in Figure 19. This suggests that this model should be used with caution for small droplet as well. Even if errors on the liquid phase do not impact the gaseous profiles, an inaccurate description of the liquid phase could impact

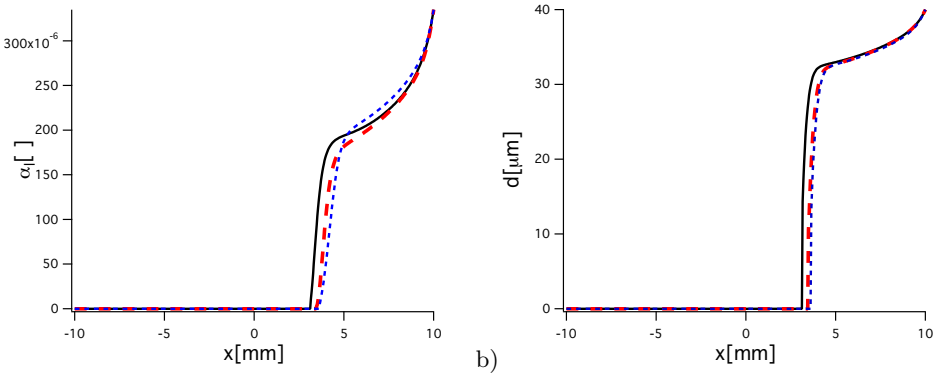

a) b)

FIGURE 10. Case REF: a) liquid volume fraction and b) droplet diameter as a function of the position for full (black full line), equilibrium (red dashed line), and equal diffusivity (blue dotted line) models.

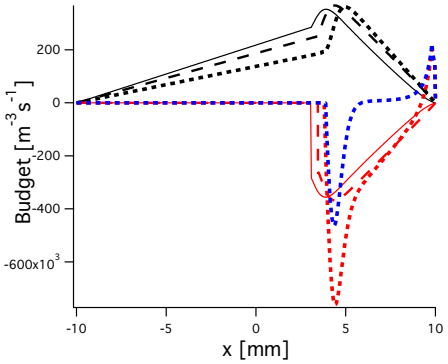

FIGURE 11. Case REF: radial flux (black line), axial flux (red line) for full (full line), equilibrium (dashed line) and equal diffusivity approximation (dotted line). The additional diffusion term for equal diffusivity approximation is added in blue.

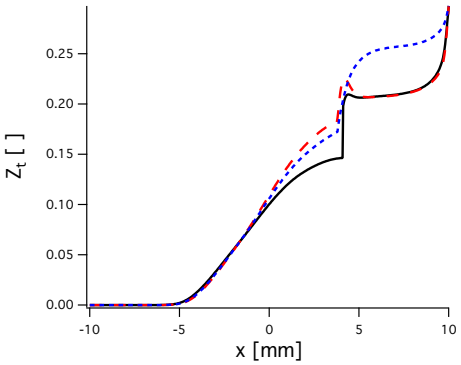

FIGURE 12. Case SMALL: total mixture fraction versus axial position for full (black full line), equilibrium (red dashed line), and species-like (blue dotted line) models.

the flame structure whenever most of the evaporation takes place in the flame reaction zone.

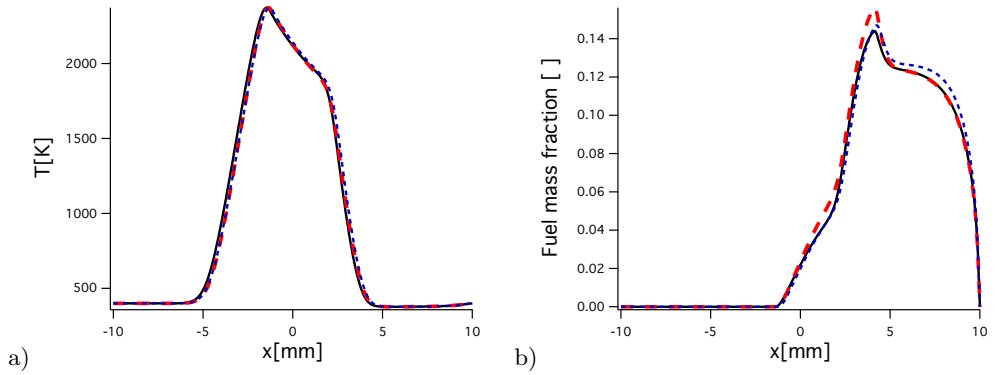

FIGURE 13. Case SMALL: a) gas temperature and b) fuel mass fraction as a function of the position for full (black full line), equilibrium (red dashed line) and species-like (blue dotted line) models.

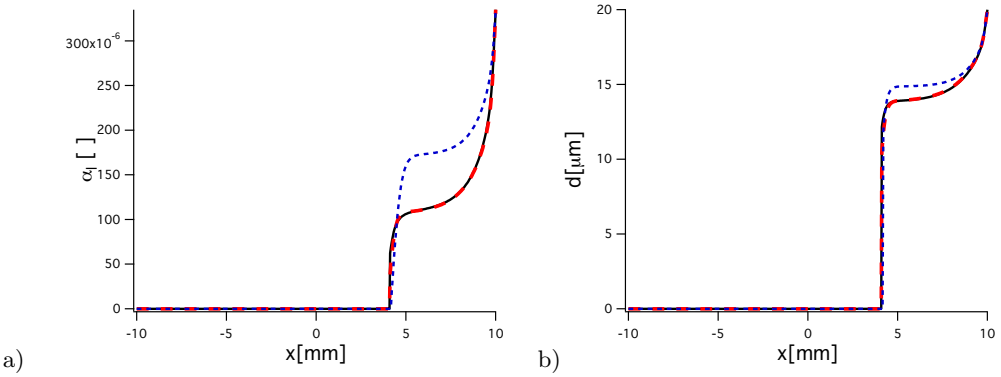

FIGURE 14. Case SMALL: a) liquid volume fraction and b) droplet diameter as a function of the position for full (black full line), equilibrium (red dashed line) and species-like (blue dotted line) models.

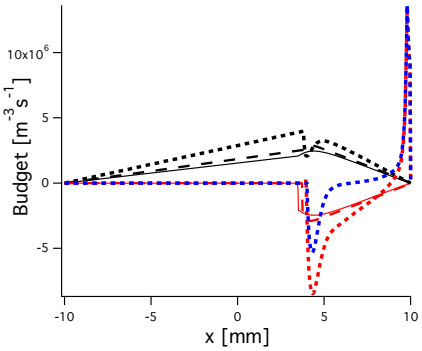

FIGURE 15. Case SMALL: radial flux (black line), axial flux (red line) and additional diffusion (blue line) for full (full line), equilibrium (dashed line) and equal diffusivity approximation (dotted line).

5.3. *Large diameter*

Finally, we consider a case with larger droplets, corresponding to a diameter of 60 μm. The solution is plotted in Figs. 16-18. As in the previous cases, the equal diffusivity

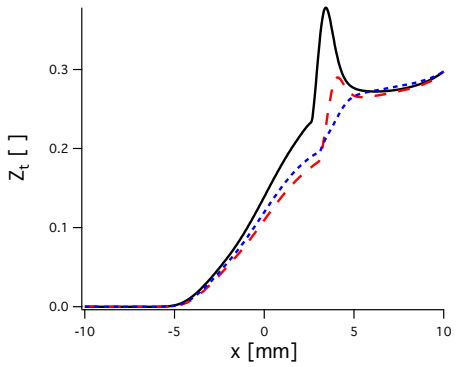

FIGURE 16. Case LARGE: total mixture fraction versus axial position for full (black full line), equilibrium (red dashed line) and species-like (blue dotted line) models.

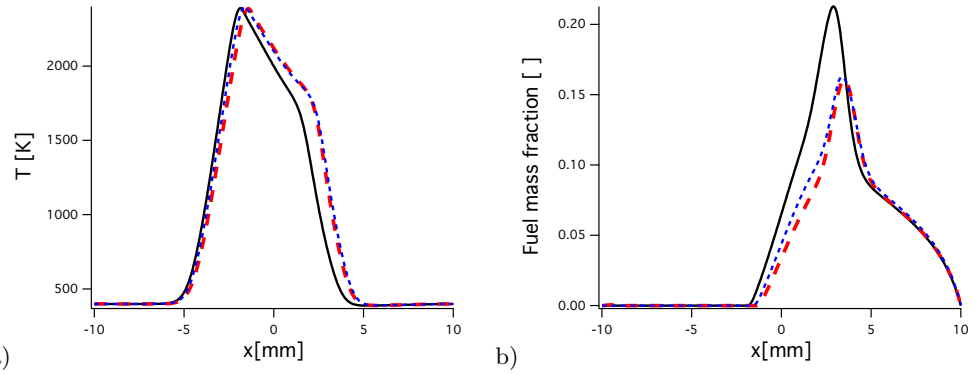

FIGURE 17. Case LARGE: a) gas temperature and b) fuel mass fraction as a function of the position for full (black full line), equilibrium (red dashed line) and species-like (blue dotted line) models.

model is again the only model with a monotonic mixture fraction. Here the equilibrium assumption has a direct impact, shifting the temperature profile closer to the injection location. Furthermore, the maximum gaseous fuel mass fraction is highly impacted by this assumption, and the full evaporation of all droplets occurs closer to the injection compared to the full model. In fact, equilibrium and equal diffusivity approximations give similar results. This is confirmed in Figure 19: the diffusion term is always smaller than every other contribution, and the main limitation is the equilibrium assumption.

6. Conclusions and perspectives

In this work, the possibility of formulating spray flame equations in the mixture fraction space has been discussed. For spray flames, the classical mixture fraction definition based on gaseous carbon atoms is no longer applicable because it is not monotonic, avoiding the use of the coordinate transformation from physical to mixture fraction space. To address this issue, a convenient way is to take into account the liquid carbon atoms in the mixture fraction definition. The behavior of this definition of the mixture fraction has been investigated. Results on a spray flame show that using this definition does not circumvent the non-monotonicity of the mixture fraction. To overcome this issue,

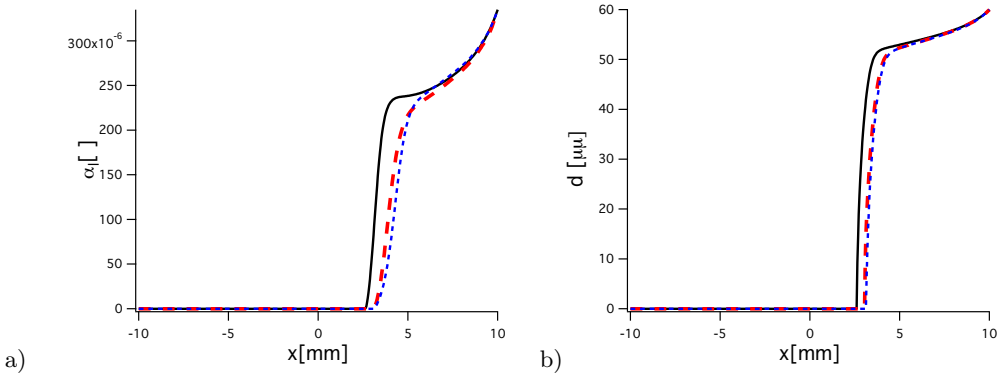

FIGURE 18. Case LARGE: a) liquid volume fraction and b) droplet diameter as a function of the position for full (black full line), equilibrium (red dashed line) and species-like (blue dotted line) models.

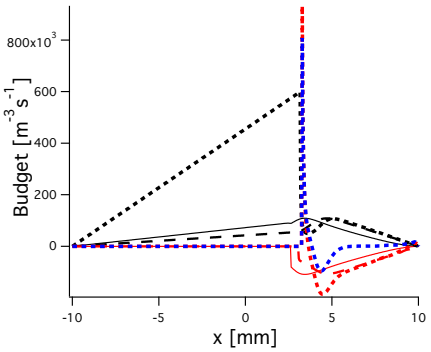

FIGURE 19. Case LARGE: radial flux (black line), axial flux (red line) and additional diffusion (bleu line) for full (full line), equilibrium (dashed line) and equal diffusivity approximation (dot-dashed line).

two models are proposed and investigated: the equilibrium model, for which the liquid velocity is the same as the gas velocity, and the equal diffusivity approximation, for which the liquid is treated as a gaseous species, having the same velocity as the gas phase and an additional diffusion term equivalent to that of the gaseous species. Results showed that only the equal diffusivity approximation is able to preserve the monotonicity of the total mixture fraction. This model gives satisfactory results for small droplet Stokes number. This result, however, is largely attributed to the fact that droplets evaporate before reaching the flame reaction zone. Since this model greatly affects the liquid volume fraction, if evaporation takes place in the flame, the impact of the model would be more significant. Thus, it can be concluded that describing spray flame structures in a mixture fraction is not straightforward. The classical gaseous definition is not sufficient, and even taking the liquid carbon atoms into account in this definition does not ensure monotonicity. Thus new definitions of the mixture fraction are needed and these will be investigated as part of our future studies.

REFERENCES

Bilger, R. 2011 A mixture fraction framework for the theory and modeling of droplets and sprays. *Combust. Flame* **158**, 191–202.

Bilger, R. W. 1988 The structure of turbulent non premixed flames. In *22nd Symp. (Int.) on Combustion*, pp. 475–488. The Combustion Institute, Pittsburgh.

Darabiha, N. & Candel, S. 1992 The influence of the temperature on extinction and ignition limits of strained hydrogen-air diffusion flames. *Combust. Sci. Tech.* **86**, 67–85.

Darabiha, N., Lacas, F., Rolon, J. & Candel, S. 1993 Laminar counterflow spray diffusion flames: A comparison between experimental results and complex chemistry calculations. *Combust. Flame* **95**, 261–275.

Franzelli, B., Fiorina, B. & Darabiha, N. 2013 A tabulated chemistry method for spray combustion. *Proc. Combust. Inst.* **34**, 1659–1666.

Franzelli, B., Riber, E., Sanjosé, M. & Poinsot, T. 2010 A two-step chemical scheme for keroseneair premixed flames. *Combust. Flame* **157** (7), 1364–1373.

Hollmann, C. & Gutheil, E. 1998 Diffusion flames based on a laminar spray flame library. *Combust. Sci. Tech.* **135** (1-6), 175–192.

Kuo, K. 1986 *Principles of Combustion*. New York: John Wiley.

Luo, K., Pitsch, H., Pai, M. & Desjardins, O. 2011 Direct numerical simulations and analysis of three-dimensional n-heptane spray flames in a model swirl combustor. *Proc. Combust. Inst.* **33**, 667–674.

Sirignano, W. A. 1983 Fuel droplet vaporisation and spray combustion theory. *Prog. Energy Comb. Sci.* **9**, 291–322.

Spalding, D. B. 1953 The combustion of liquid fuels. In *4th Symp. (Int.) on Combustion*, pp. 847–864. The Combustion Institute, Pittsburgh.